AGU PUBLICATIONS

JGR

Journal of Geophysical Research: Biogeosciences

RESEARCH ARTICLE
10.1002/2015JG003130

Key Points:
- Incorporating dormancy reduces oscillation in microbial biomass
- Biogeochemical controls on microbial dynamics are scale dependent
- Soil nutrient is a major factor at regional scales

Supporting Information:
- Supporting Information S1

Correspondence to:
Q. Zhuang,
qzhuang@purdue.edu

Citation:
He, Y., J. Yang, Q. Zhuang, J. W. Harden, A. D. McGuire, Y. Liu, G. Wang, and L. Gu (2015), Incorporating microbial dormancy dynamics into soil decomposition models to improve quantification of soil carbon dynamics of northern temperate forests, *J. Geophys. Res. Biogeosci.*, *120*, doi:10.1002/2015JG003130.

Received 1 JUL 2015
Accepted 18 NOV 2015
Accepted article online 20 NOV 2015

Incorporating microbial dormancy dynamics into soil decomposition models to improve quantification of soil carbon dynamics of northern temperate forests

Yujie He[1], Jinyan Yang[2,3], Qianlai Zhuang[1,4], Jennifer W. Harden[5], Anthony D. McGuire[6], Yaling Liu[1], Gangsheng Wang[7], and Lianhong Gu[8]

[1]Department of Earth, Atmospheric, and Planetary Sciences, Purdue University, West Lafayette, Indiana, USA, [2]Warnell School of Forestry and Natural Resources, University of Georgia, Athens, Georgia, USA, [3]Center for Ecological Research, Northeast Forestry University, Harbin, China, [4]Department of Agronomy, Purdue University, West Lafayette, Indiana, USA, [5]U.S. Geological Survey, Menlo Park, California, USA, [6]Alaska Cooperative Fish and Wildlife Research Unit, U.S. Geological Survey, University of Alaska Fairbanks, Fairbanks, Alaska, USA, [7]Climate Change Science Institute and Environmental Sciences Division, Oak Ridge National Laboratory, Oak Ridge, Tennessee, USA, [8]Environmental Sciences Division, Oak Ridge National Laboratory, Oak Ridge, Tennessee, USA

Abstract Soil carbon dynamics of terrestrial ecosystems play a significant role in the global carbon cycle. Microbial-based decomposition models have seen much growth recently for quantifying this role, yet dormancy as a common strategy used by microorganisms has not usually been represented and tested in these models against field observations. Here we developed an explicit microbial-enzyme decomposition model and examined model performance with and without representation of microbial dormancy at six temperate forest sites of different forest types. We then extrapolated the model to global temperate forest ecosystems to investigate biogeochemical controls on soil heterotrophic respiration and microbial dormancy dynamics at different temporal-spatial scales. The dormancy model consistently produced better match with field-observed heterotrophic soil CO_2 efflux (R_H) than the no dormancy model. Our regional modeling results further indicated that models with dormancy were able to produce more realistic magnitude of microbial biomass (<2% of soil organic carbon) and soil R_H (7.5 ± 2.4 Pg C yr^{-1}). Spatial correlation analysis showed that soil organic carbon content was the dominating factor (correlation coefficient = 0.4–0.6) in the simulated spatial pattern of soil R_H with both models. In contrast to strong temporal and local controls of soil temperature and moisture on microbial dormancy, our modeling results showed that soil carbon-to-nitrogen ratio (C:N) was a major regulating factor at regional scales (correlation coefficient = −0.43 to −0.58), indicating scale-dependent biogeochemical controls on microbial dynamics. Our findings suggest that incorporating microbial dormancy could improve the realism of microbial-based decomposition models and enhance the integration of soil experiments and mechanistically based modeling.

1. Introduction

Soil has always been a focus of climate change studies due to its large carbon (C) stocks—the global soil organic C (SOC) stock is at least four times greater than atmospheric C [*Irvine and Law*, 2002; *Jobbágy and Jackson*, 2000], and soil respiration is the second largest flux between the biosphere and the atmosphere following photosynthesis [*Raich and Potter*, 1995]. Therefore, soil C dynamics plays a key role in net C sequestration of terrestrial ecosystems and is essential to our understanding of biogeochemical cycles and its climate-C interactions [*IPCC*, 2013].

Recent comprehensive analyses have shown that there are notable limitations of traditional first-order decomposition algorithms in current Earth system models. Those decomposition models are not able to capture the spatial distributions of SOC stocks and primary drivers of SOC dynamics [*Todd-Brown et al.*, 2013], while microbial-based soil organic matter decomposition models have been increasingly used at both site- and global-scale studies [*Allison et al.*, 2010; *He et al.*, 2014b; *Wieder et al.*, 2013], although more rigorous examination of these models is still needed [*Li et al.*, 2014]. The current generation of microbial-based decomposition models usually features a common framework where enzyme production and microbial physiology are associated with total microbial biomass (MIC), which has a direct coupling with SOC enzymatic decomposition.

A key microbial life history trait that is usually lacking in these models is microbial dormancy. Dormancy is a common, bet-hedging strategy used by microorganisms when environmental conditions limit growth and reproduction [*Lennon and Jones*, 2011]. When microorganisms are confronted with unfavorable conditions, they may enter a reversible state of low metabolic activity and resuscitate when favorable conditions occur. Microorganisms in this state of reduced metabolic activity are not able to drive biogeochemical processes such as soil CO_2 production; therefore, only active microorganisms are involved in utilizing substrates in soils [*Blagodatskaya and Kuzyakov*, 2013]. Although some studies have explicitly incorporated dormancy into models [*Ayati*, 2012; *Wirtz*, 2003], they are mostly confined to incubation experiments, and applications of microbial models in natural environments generally do not consider dormancy.

There are four motivations that led to the inception of this study to represent dormancy in microbial-based decomposition models. First, the current coupled SOC-MIC structure leads to oscillatory behavior of soil organic and microbial C pools with unrealistically large amplitudes of interannual variation [*Y. Wang et al*., 2014; *Wieder et al*., 2013]; thus, incorporating dormancy may structurally improve model realism. Second, there is a scale mismatch in current measurement procedures of microbial biomass since different portions of microbial biomass are actually measured. For example, substrate-induced respiration and fumigation techniques measure the total microbial biomass when the conversion factor is used, whereas direct microscopy combined with cell staining such as fluorescence in situ hybridization measures the active portion of total biomass [*Blagodatskaya and Kuzyakov*, 2013] Along this line, the aforementioned inconsistency may pose challenges in data-model integration and in microbial model comparisons and evaluation. Finally, the transition between dormant and active states of microbes can be fast (in the order of hours to days) with substantial magnitude change (e.g., an order of magnitude) in the portion of active biomass and the relative abundance of different phylogenetically clustered microbial groups; however, these transitions usually feature little change in total microbial biomass [*Hagerty et al*., 2014; *Placella et al*., 2012]. Thus, total microbial biomass may not be a sufficient indicator of microbial activities as opposed to the more responsive active portion of microbial biomass.

In this study, we hypothesize that (1) a microbial model incorporated with dormancy would outperform the model without dormancy at site-level parameterization and (2) a microbial model with dormancy would produce more realistic microbial biomass and soil R_H on both site and regional scales. We compared two microbial models with and without representation of dormancy to examine the site and regional patterns of the estimated SOC and microbe-related variables. The model parsimony and overfitting potentials were also considered during the comparison. We also discuss the primary controls on microbial and SOC dynamics at different tempospatial scales.

2. Methods

2.1. Model Description

In this study, dormancy was incorporated into an existing microbial-enzyme conceptual framework described by *Allison et al*. [2010], in which an Arrhenius formulation of temperature sensitivity was replaced with a simplified temperature-sensitive Q_{10} function ($Q_{10}^{\frac{temp-15}{10}}$) to reduce the number of model parameters. The reversible transition between dormant and active states of microbial biomass is assumed to be controlled by environmental cues—directly accessible substrates, as demonstrated in *G. Wang et al*. [2014]. We integrate *Davidson et al*.'s [2012] conceptual framework of quantifying concentration of soluble C substrates that are directly accessible for microbial assimilation, thus building a direct linkage between environmental factors with microbial state transitions. Substrate quality is also reflected in the model through a generic index of soil C:N ratio [*Manzoni et al*., 2008], and the assimilation of substrate by microorganisms is assumed to be regulated by the C:N ratio of microbial biomass and that of the soil. We apply the model to simulate the top 30 cm of the soil due to data availability for site validation. The equations for the model with microbial dormancy are as follows:

$$\frac{dSOC}{dt} = Input - \overbrace{V_{max} Q_{10enz}^{\frac{temp-15}{10}} ENZ \frac{SOC}{K_m + SOC}(120 - CN_{soil})}^{Decomposition} \quad (1)$$

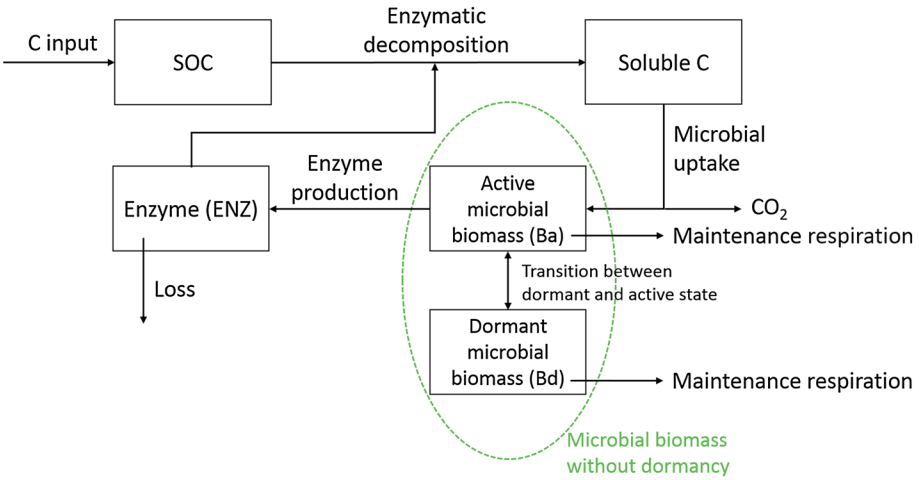

Figure 1. Schematic diagram of the conceptual representation of the dormancy model.

$$\frac{\mathrm{dSolubleC}}{\mathrm{d}t} = \mathrm{Decompostion} - \overbrace{\frac{1}{Y_g}\frac{\phi}{\alpha} m_R Q_{10enz}^{\frac{temp-15}{10}} B_a \left(\frac{CN_{soil}}{CN_{mic}}\right)^{0.6}}^{\text{Microbial uptake}} + B_a r_{death} + ENZ r_{loss} \quad (2)$$

$$\frac{\mathrm{d}B_a}{\mathrm{d}t} = \left(\frac{\phi}{\alpha} - 1\right) m_R Q_{10mic}^{\frac{temp-15}{10}} B_a \left(\frac{CN_{soil}}{CN_{mic}}\right)^{0.6} \overbrace{-(1-\phi) m_R Q_{10mic}^{\frac{temp-15}{10}} B_a}^{\text{Transition from active to dormant}} \overbrace{+\phi m_R Q_{10mic}^{\frac{temp-15}{10}} B_d}^{\text{Transition from dormant to active}} - B_a r_{prod} - B_a r_{death} \quad (3)$$

$$\frac{\mathrm{d}B_d}{\mathrm{d}t} = -\beta m_R Q_{10mic}^{\frac{temp-15}{10}} B_d + (1-\phi) m_R Q_{10mic}^{\frac{temp-15}{10}} B_a - \phi m_R Q_{10mic}^{\frac{temp-15}{10}} B_d \quad (4)$$

$$\frac{\mathrm{dENZ}}{\mathrm{d}t} = B_a r_{prod} - ENZ r_{loss} \quad (5)$$

where "Input" denotes the overall C input to the soil system, including litterfall and root exudates; state variables are SOC, SolubleC, B_a, B_d, and ENZ, corresponding to SOC content, soluble C content, microbial biomass in active and dormant states, and enzyme C (mg C cm^{-2}), respectively (Figure 1); temp is soil temperature at each time step t; ϕ is the directly accessible substrate for microbial assimilation, calculated based on Michaelis-Menten kinetics formulated as $\phi = \frac{\mathrm{SolubleC} \times D_{liq} \times \theta^3}{K_s + \mathrm{SolubleC} \times D_{liq} \times \theta^3}$, where D_{liq} is a diffusion coefficient of the substrate in the liquid phase (determined by assuming all soluble substrate is directly accessible at the reaction site, formulated as $D_{liq} = 1/(1 - \mathrm{BD}/\mathrm{PD})^3$; BD is the bulk density and PD is the soil particle density); θ is the volumetric soil moisture content; and K_s is corresponding Michaelis constant [*Davidson et al.*, 2012]. A detailed description for other parameters is summarized in Table 1. The soil heterotrophic respiration generated from this conceptual model is expressed as

$$R_H = m_R Q_{10enz}^{\frac{temp-15}{10}} B_a + \beta m_R Q_{10mic}^{\frac{temp-15}{10}} B_d + \left(\frac{1-Y_g}{Y_g}\right)\frac{\phi}{\alpha} m_R Q_{10enz}^{\frac{temp-15}{10}} B_a \left(\frac{CN_{soil}}{CN_{mic}}\right)^{0.6} \quad (6)$$

where the first two terms are maintenance respiration from the active and dormant microorganisms, respectively. The last term is the CO_2 produced during the microbial uptake of substrate. Adding up equations (3) and (4) shown above gives the model without dormancy (Figure 1). Note that the dormancy model only introduces two more free parameters than the no dormancy model: (1) the ratio of dormant microbial maintenance rate to that of active biomass (β), which has a well-defined range and has marginal contribution to the overall CO_2 efflux, and (2) the initial active fraction (r_0), to which C dynamics is not sensitive because of the fast response of microbes to the environment (Table 1). Sensitivity analysis showed that simulated SOC and microbial biomass were not sensitive to these two parameters (Figure S1 in the

Table 1. Description of Parameters Used in the Model and the Prior Used in Inverse Modeling[a]

Parameter	Description	Prior/Value (Dormancy Model)	Prior/Value (No Dormancy Model)	Notes and Citations
α	Maintenance weight, $m_R/(\mu_G + m_R)$, where μ_G is the specific growth rate (h^{-1})	[0.01, 0.5]	[0.005, 0.05]	*G. Wang et al.* [2014]
β	Ratio of dormant microbial maintenance rate to m_R	[0.0005, 0.005]	-	*G. Wang et al.* [2014], *Blagodatskaya and Kuzyakov* [2013]
m_R	Specific maintenance rate for active biomass (h^{-1})	[0.001, 0.08]	[0.0001, 0.008]	*G. Wang et al.* [2014], *Schimel and Weintraub* [2003], *Blagodatskaya and Kuzyakov* [2013]
K_s	Half-saturation constant for directly accessible substrate (mg C cm^{-2})	[0.01, 10]	Same	Calculated based on approximate range of SolubleC/SOC ratio of 1e−4 to 1e−3 [*Davidson et al.*, 2012] and reported K_s for substrate breakdown of 72 mg kg^{-1} soil [*Xu et al.*, 2014]
K_m	Half-saturation constant for enzymatic decay of SOC (mg C cm^{-2})	[200, 1000][b]	Same	Assuming SOC is not at saturation for enzymatic decay [*Schimel and Weintraub*, 2003]
V_{max}	Maximum SOC decay rate	[1e−4, 5e−3]	Same	Calculated based on the magnitude of litter input C
r_{prod}	Enzyme production rate of active microorganism (h^{-1})	[1e−4, 8e−4]	[1e−5, 8e−5]	*Schimel and Weintraub* [2003] assumes 5% of the C uptake by microorganism is allocated to exoenzyme production (d^{-1}). This is equivalent to an hourly rate of 2e−3 h^{-1}; the typical hourly uptake rate in our model is ~0.3 per microbial biomass
r_{loss}	Enzyme loss rate (h^{-1})	[0.0005, 0.002]	Same	*Allison et al.* [2010], *Schimel and Weintraub* [2003]
r_{death}	Potential rate of microbial death (h^{-1})	[2e−4, 2e−3]	[2e−5, 2e−4]	*Allison et al.* [2010], *Xu et al.* [2014]
Q_{10enz}	Temperature effects on enzyme activity (rate change per 10 °C increase in temperature). Based on 6% rate increase per degree Celsius	1.79	Same	*Purich* [2009]
Q_{10mic}	Temperature effects on microbial metabolic activity (rate change per 10 °C increase in temperature). Based on 0.65 eV activation energy for soils	[1.5, 3.5]	Same	*Yvon-Durocher et al.* [2012]
Y_g	True growth yield, or carbon use efficiency	[0.3, 0.7]	Same	*Sinsabaugh et al.* [2013]
Y_{g_slope}	Temperature sensitivity of Y_g per degree Celsius increase	−0.012	Same	*German et al.* [2012]
Initial active fraction (r_0)	Active portion of microbial biomass	[0.05, 0.3]	-	*Lennon and Jones* [2011]

[a]The value is given if the parameter is predefined to be a constant and is not used in inverse modeling. Parameters that are per microbial biomass based have different priors for the dormancy and no dormancy models. Note that the model simulates the top 30 cm of soil.
[b]Lower bound of 50 is used for US-MOz due to its low SOC content.

supporting information). In addition, inclusion of these two parameters does not significantly alter the correlation structure between parameters (Figure S2); however, the structural changes induced by the dormancy mechanism may be more notable.

Environmental factors such as substrate availability are often thought to be the primary triggering mechanism ending dormancy [*Lennon and Jones*, 2011]. Therefore, we adopted the formulation described in *G. Wang et al.* [2014], where the transition between active and dormant states of microorganisms is scaled linearly with substrate availability (ϕ), which is a Michaelis-Menten function of water availability, and the direction of the net transition is determined by the balance of maintenance metabolic requirement.

We recognize that our model only simulates C dynamics, and decomposition is effectively influenced by various nutrients through kinetic and stoichiometric constraints that are not explicitly represented in this model [*Sinsabaugh et al.*, 2013]. Instead of using a more sophisticated modeling framework, we introduced

Journal of Geophysical Research: Biogeosciences

10.1002/2015JG003130

Table 2. Calibration Sites That Are Used in This Study, Including Three Sites From Northeastern China and Three AmeriFlux Sites From the Coterminous U.S[a]

	Mixed Deciduous Forest (CN-Mixed)	Oak Forest (CN-Oak)	Larch Plantation (CN-Lar)	Marys River Fir (US-MRf)	Metolius Intermediate Pine (US-Me2)	Missouri Ozark (US-MOz)
Latitude, longitude	45.33–45.42N, 127.50–127.56E	45.33–45.42N, 127.50–127.56E	45.33–45.42N, 127.50–127.56E	44.65N, 123.55W	44.45N, 121.56W	38.74N, 92.20W
Elevation (m above sea level)[1]	400	400	400	263	1253	219
MAT, MAP[1]	2.8 °C, 700 cm	2.8 °C, 700 cm	2.8 °C, 700 cm	9.0 °C, 1350 mm	10 °C, 480 mm	12.8 °C, 940 mm
Vegetation (IGBP)	Mixed forest	Deciduous broadleaf forest	Deciduous needleleaf forest	Evergreen needleleaf forest	Evergreen needleleaf forest	Deciduous broadleaf forest
Dominant species in overstory[1]	*Tilia amurensis* Rupr.; *Juglans mandshurica* Maxim.	*Quercus mongolica* Fisch;	*Larix gmelinii* Rupr.	*Pseudotsuga menziesii* (Mirb.) Franco (Douglas fir)	*Pinus ponderosa* (ponderosa pine)	*Quercus alba* L. (white oak), *Quercus velutina* Lam. (black oak)
Soil type[2]	Sandy loam	Sandy loam	Sandy loam	Sandy loam[b]	Sandy loam	Silt loam
Clay[2]	-	-	-	-	7	21
Sand[2]	-	-	-	-	67	4
Silt[2]	-	-	-	-	26	75
Soil C:N[3]	13.6	20.6	15.8	23.86[b]	23.86	15.8[b]
SOC fraction (%)[4]	9.7	7.6	4.8	1.2[b]	1.2	0.97
Bulk density (g cm^{-3})[5]	0.63	0.58	1.01	1.15[b]	1.15	1.37
Microbial biomass C (mg kg^{-1})[6]	1950	1050	900	-	-	-
Microbial biomass N (mg kg^{-1})[6]	210	110	90	-	-	-
Microbial C:N[6]	9.3	9.6	10	-	-	-
MIC/SOC[6]	0.013	0.011	0.009	0.016	0.016	0.99
Citations	*C. Wang et al.* [2006]; *Fu et al.* [2009]; *Yang and Wang* [2005]; *Liu and Wang* [2010]	*C. Wang et al.* [2006]; *Fu et al.* [2009]; *Yang and Wang* [2005]; *Liu and Wang* [2010]	*C. Wang et al.* [2006]; *Fu et al.* [2009]; *Yang and Wang* [2005]; *Liu and Wang* [2010]	*Thomas et al.* [2009]; *Xu et al.* [2013]	*Irvine and Law* [2002]; DOI: 10.3334/CDIAC/amf.US-Me2.b; *Xu et al.* [2013]	*Irvine and Law* [2002]; *McFarlane et al.* [2013]; DOI: 10.3334/CDIAC/amf.US-Moz.b; *Xu et al.* [2013]

[a]Soil properties are based on the total element content or measurements in the top 30 cm of soil.
[b]Values are not reported in the literature, average of the same ecosystem type is used for substitution.

a temperature- and population size-dependent scaling factor on the potential microbial death rate, formulated as $1.5^{\frac{\text{temp}-15}{10}} \times \frac{B_a}{\text{SOC} \times 0.025}$, where a metabolic temperature sensitivity of 1.5 and a population capacity of 2.5% of SOC are assumed for temperate forest soils [*Xu et al*., 2013; *Yvon-Durocher et al*., 2012]. This multiplier is used to modify the parameter r_{death} and implicitly represents competition for nutrients and downregulates microbial growth.

2.2. Model Calibration and Validation

We calibrated the model at six different temperate forest sites in northeastern China (three) and conterminous U.S. (three) with a latitudinal span of 38–45°N using a global optimization algorithm known as the SCE-UA (shuffled complex evolution) [*Duan et al*., 1994] (Table 2). An ensemble of 100 independent optimization runs were performed based on prior ranges from the literature (Table 1), each using different random number seeds to determine the successive evolution steps. The resulting parameter distribution was used for the correlation analysis mentioned above and for spatial extrapolations. The three northeastern China sites (CN-Mixed, CN-Oak, and CN-Lar) were all trenched plots (no litter input) with monthly measured R_H, soil temperature, and gravimetric soil moisture content at 10 cm from 2004 to 2007 [*C. Wang et al*., 2006]. The three U.S. sites (US-MRf, US-Me2, and US-MOz) are part of the AmeriFlux network. The level 2 (gap-filled) eddy covariance data with half-hourly measured soil temperature (at 10 cm, °C), volumetric soil moisture content (at 10 cm, %; VSM), and automated soil chamber-measured soil respiration (μmol m^{-2} s^{-1}) were used for this study [*Irvine and Law*, 2002]. For the U.S. sites, approximately 50% of soil respiration was assumed to be R_H [*Hanson et al*., 2000]. Litterfall was assumed to be a fixed proportion (0.3) of net primary production (NPP) based on field litterfall measurements and remote sensing-derived NPP estimation, and we assume NPP/GPP = 0.45 (gross primary production, GPP) based on the eddy covariance measurements at the US-MRf site. GPPs at the US-Me2 and US-MRf sites (see Table 2) were also obtained from level 2 data but were not available for the US-MOz site. Therefore, for the R_H measurement period (2004–2007), we used level 4 gap-filled net ecosystem exchange (NEE) and we calculated GPP based on NEE and meteorological data using an online flux partitioning tool (http://www.bgc-jena.mpg.de/~MDIwork/eddyproc/upload.php) [*Lasslop et al*., 2010]. Site-level state variables (e.g., SOC content, microbial biomass, and soil C:N) served as initial states for the model calibration. Microbial biomass data are not available at the three U.S. sites (Table 2); thus, the MIC/SOC ratio of the same forest type reported in *Xu et al*. (2013) was used and biomass was calculated based on SOC content. Note that parameter priors that were microbial biomass specific were rescaled based on the active portion of microbial biomass (Table 1). At each site, the first 75% of total available data were used for calibration and the remaining was used for validation. Model evaluation statistics were calculated using the whole data series.

2.3. Data Sources for Spatial Extrapolation

We used the above calibrated ecosystem-specific parameters and extrapolated to the whole temperate forest region defined as the latitudinal band from 25°N to 50°N. We did not include the Southern Hemisphere due to lack of calibration site located in the region. The average parameters of the corresponding forest types are used for each forest type involved in the latitudinal band. Forest land cover information was extracted from the Moderate Resolution Imaging Spectroradiometer land cover product (MCD12C1) for the period 2000–2012, and annual mean land cover distribution was used. The original 0.05° × 0.05° (lon × lat) resolution grid was aggregated to 0.5° × 0.5° using a majority resampling approach to best preserve the spatial structure of the major classes. NPP (2000–2012, annual mean) data were extracted from MOD17A3 L4 Global 1 km product (version 55) [*Zhao and Running*, 2010]. The original data were aggregated to 0.5° × 0.5° using the areal mean. Soil physical properties and organic C and N content of the top 30 cm were obtained from gridded Global Soil Data Set for use in Earth System Models (GSDE) data set [*Shangguan et al*., 2014]. Particle density was calculated based on bulk density and porosity, and porosity was estimated using volumetric soil moisture (VSM) at -10 kPa (provided in GSDE). Specifically, we assumed saturated VSM is the same as VSM at −10 kPa for silt loam soil and we added 10% for sandy loam soil based on the soil water retention curve [*Cornelis et al*., 2005]. Soil was classified according to soil taxonomy (Soil Survey Staff, 2003) and using sand, silt, and clay content from GSDE data set. For transient simulations, we used CMIP5 historical runs (CMIP5 30 year run) initialized in year 2006 from CCSM4 land modeling realm (ensemble = r1i1p1) to retrieve soil temperature (tsl, average of top 10 cm) and soil water content in the top 10 cm (mrsos) (http://www.earthsystemgrid.org). Soil water content in mass was converted to soil volumetric moisture using relevant soil

Table 3. Model Evaluation Statistics From Best Inverse Parameter Estimation for Dormancy and No Dormancy Model at the Six Temperate Forest Sites[a]

Model	RMSE (SD)** (mg C cm^{-2} h^{-1})	Adjusted R^2 (SD)***	NS Coefficient**	Seasonal MIC Amplitude (mg C cm^{-2})**	Adjusted RMSE (mg C cm^{-2} h^{-1})*
			Dormancy model		
CN-Mixed	0.0037	0.58	0.54	2.82	0.0052
CN-Oak	0.0030	0.73	0.72	0.92	0.0044
CN-Lar	0.0017	0.74	0.72	0.68	0.0023
US-MRf	0.0011	0.76	0.75	1.72	0.0011
US-Me2	0.0011	0.66	0.63	1.97	0.0011
US-MOz	0.0018	0.49	0.42	1.14	0.0018
			No dormancy model		
CN-Mixed	0.0080	0.29	−1.39	5.79	0.010
CN-Oak	0.0044	0.38	−1.13	6.68	0.0059
CN-Lar	0.0031	0.49	0.32	7.60	0.0039
US-MRf	0.0009	0.70	0.69	2.39	0.0009
US-Me2	0.0019	0.58	0.29	3.60	0.0019
US-MOz	0.0045	0.11	−2.5	2.80	0.0045

[a]NS is the Nash-Sutcliffe model efficiency coefficient. Adjusted RMSE is a measure of model goodness of fit adjusted for the number of free parameters in the model. The significance of the difference of metrics between the two models is tested using paired *t*-test.
*Metrics are significantly different at $p < 0.1$;
**$p < 0.05$;
***$p < 0.01$.

properties provided by the GSDE data set. Soil temperature and moisture data were interpolated from 0.9° × 1.25° to 0.5° × 0.5° using a bilinear interpolation method [*T. Wang et al.*, 2006].

2.4. Statistical Analysis

In addition to evaluating the models' capability to replicate SOC and R_H, we are also interested in the overall functional correlations between dormancy and related environmental factors as represented in the models; we choose to use simple Pearson correlation for spatial correlation analysis. The spatial extrapolation used the soil temperature and moisture profile from 2006 and ran for 3 years, and the simulation results for the last year were used for spatial grid-based and temporal correlation analyses. For model calibration and validation, we used root-mean-square error (RMSE), parameter-adjusted coefficient of determination (adj-R^2), Nash-Sutcliffe model efficiency coefficient (NS coefficient), and adjusted RMSE ($\sqrt{\frac{SSE}{n-k}}$) which accounts for model parsimony to show model performance. RMSE measures the mean difference between modeled and observed values, adj-R^2 indicates how well simulations capture the variations in the observations, and Nash-Sutcliffe coefficient denotes how well the model predictions are in comparison to model mean (same definition as the coefficient of determination R^2 used in linear regression).

3. Results

3.1. Site-Level Calibration and Validation

Both the dormancy and no dormancy models can reproduce the observed soil R_H reasonably well. The dormancy model across the six sites showed adj-R^2 over the whole measurement period ranging from 0.49 to 0.76 (Table 3), with Nash-Sutcliffe model efficiency coefficients of similar range (0.42 to 0.75). The no dormancy model performed notably worse in five out of the six sites (except US-MRf site) as adj-R^2 ranged from 0.29 to 0.58; the Nash-Sutcliffe coefficients were also much lower and were even negative at three sites (Table 3). The same pattern holds after accounting for the number of model parameters (parsimony and adjusted RMSE, Table 3). The no dormancy model performed especially poorly based on comparison to observed soil respiration well at Missouri Ozark AmeriFlux site (US-MOz) (adj-$R^2 = 0.11$), likely because the low SOC content at this site makes it more difficult to find an appropriate K_m due to its high sensitivity (see discussion in section 4.3). A paired *t*-test on root-mean-square error, adj-R^2, and Nash-Sutcliffe coefficient showed significant differences between the two models (df = 5; $p < 0.05$ for RMSE, $p < 0.01$ for adj-R^2, and

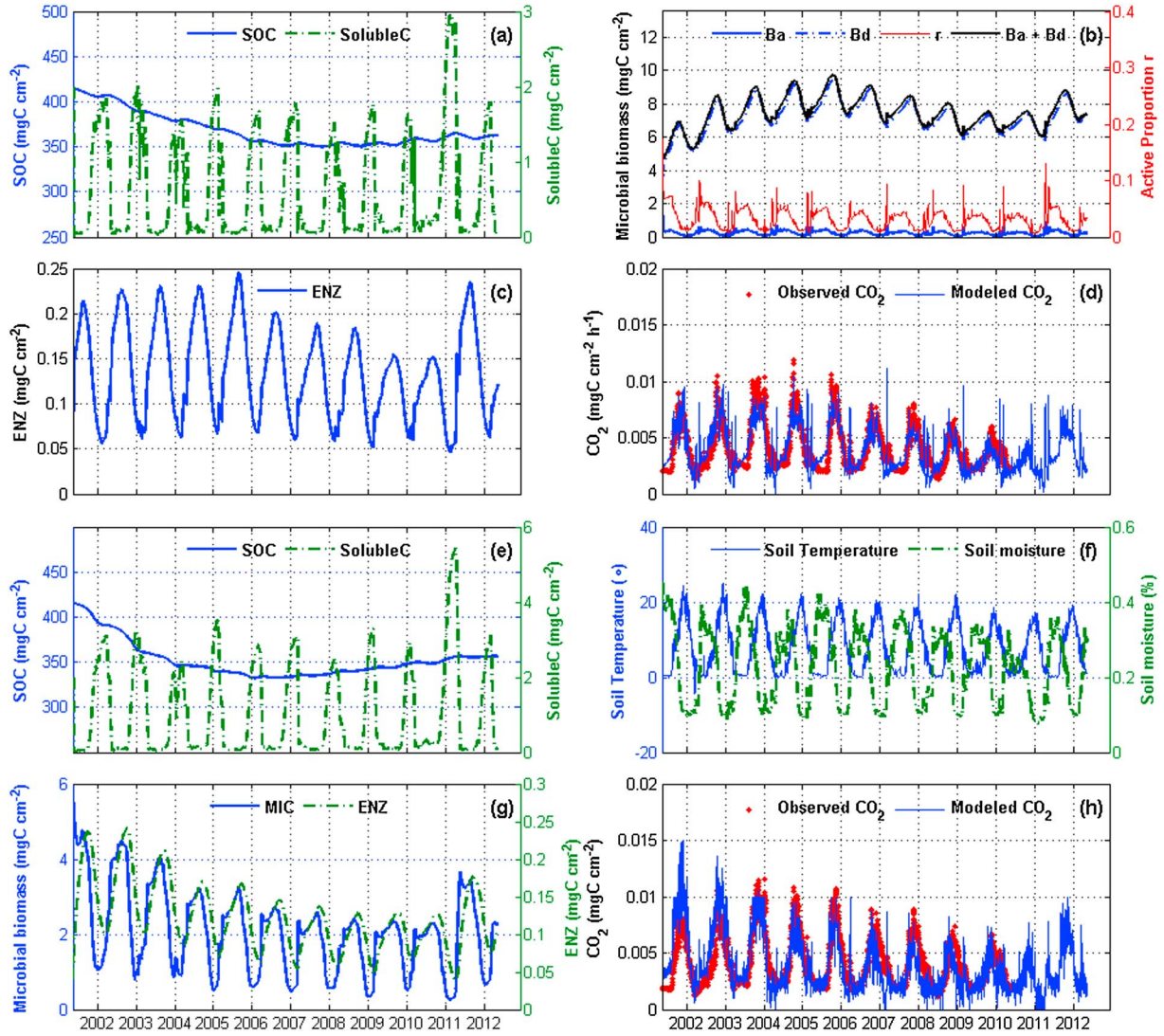

Figure 2. Modeled SOC decomposition dynamics at an AmeriFlux ponderosa pine forest in the United States (US-Me2). (a–d) Outputs from the dormancy model; (e, g, h) Outputs from the no dormancy model. (f) is the measured soil temperature and volumetric moisture content at the site. Both models reproduced observed CO_2, but there is less oscillation in microbial biomass in the dormancy model (Figures 2b and 2g), and the active fraction of microbial biomass closely tracked soil moisture conditions (Figures 2b and 2f). Legend in the figure denotes the following: Ba—active microbial biomass; Bd—dormancy microbial biomass; r—active portion of microbial biomass; MIC—total microbial biomass in the no dormancy model; ENZ—enzyme carbon.

$p < 0.05$ for Nash-Sutcliffe coefficient). Simulated dynamics of various C pools (e.g., SOC, SolubleC, ENZ, and MIC) of the two models exhibited similar patterns over time (Figures 2 and 3).

SOC at US-Me2 showed a slight decline over the course of 11 years in both models (Figures 2a and 2e), with SolubleC content showing a seasonal fluctuation antiphased with microbial biomass due to active substrate uptake during summer, thus less substrate availability, and suppressed microbial activity during winter, which led to the accumulation of substrate (Figures 2a and 2e). The active portion of microbial biomass tracked closely the changes in soil moisture, despite the dramatically different moisture regimes at the two sites, where US-Me2 site experienced a moderate drought during summer while the CN-Lar site featured benign moisture conditions for microbial decomposition (Figures 2b, 2f, 3b, and 3f). It is worth noting here that the seasonal MIC amplitude (calculated as the difference between annual maximum and minimum MIC) was always much larger (up to two times larger) in no dormancy models than in the dormancy models (Table 3 and Figures 2b, 2g, 3b, and 3g). Thus, the magnitude of the oscillations in the dormancy model is significantly smaller than in the no dormancy model (model difference df = 5, $p < 0.05$).

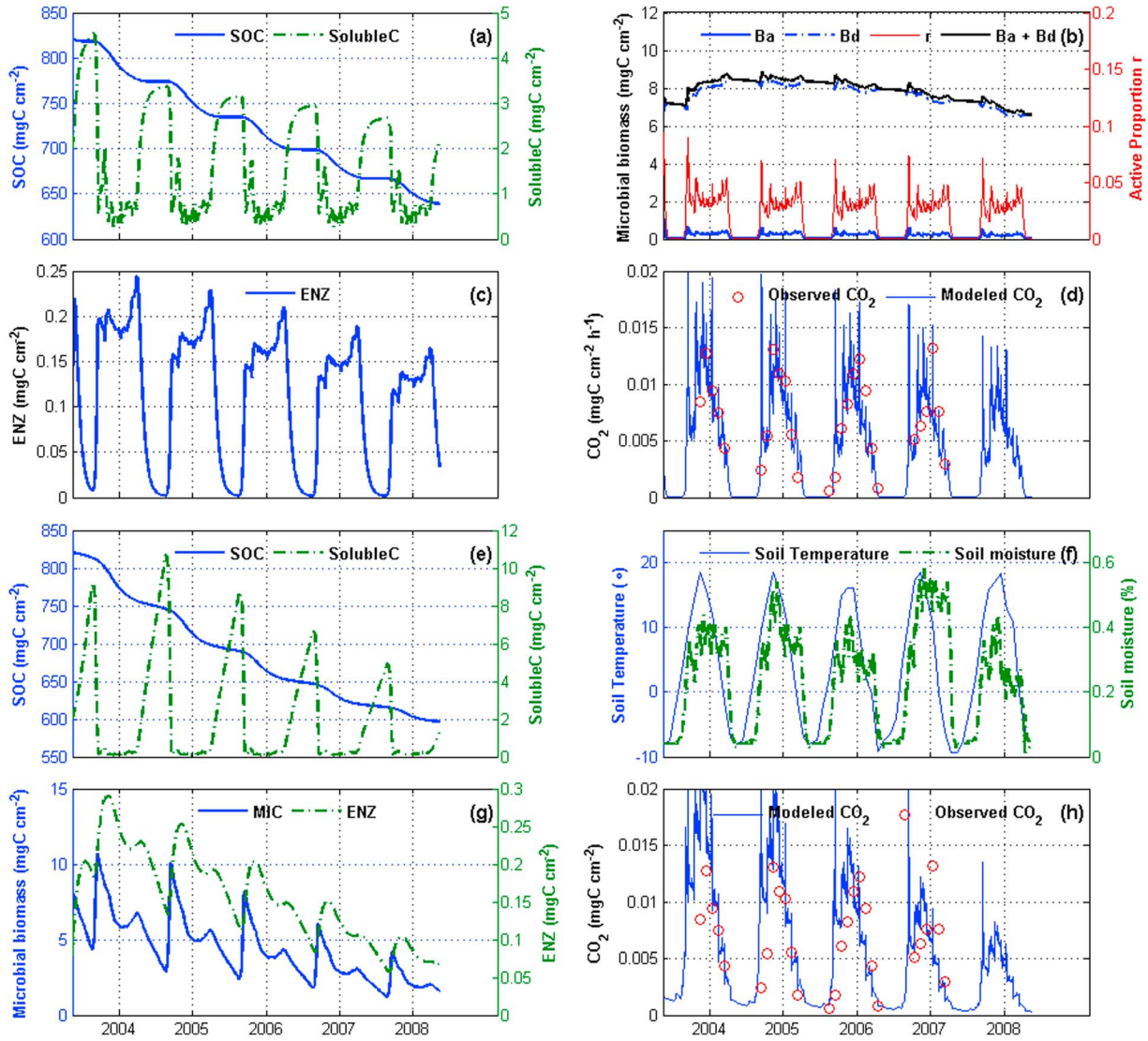

Figure 3. Modeled SOC decomposition dynamics at the larch plantation in northeastern China (CN-Lar). Note that this is a trenched plot; therefore, SOC is depleting. (a–d) Outputs from the dormancy model; (e, g, h) outputs from the no dormancy model. (f) The measured soil temperature and volumetric moisture content at the site. Both models reproduced observed CO_2, but there is less oscillation in microbial biomass in the dormancy model (Figures 3b and 3g), and the active fraction of microbial biomass closely tracked soil moisture conditions (Figures 3b and 3f). Legend in the figure denotes the following: Ba—active microbial biomass; Bd—dormancy microbial biomass; r—active portion of microbial biomass; MIC—total microbial biomass in the no dormancy model; ENZ—enzyme carbon.

3.2. Inversed Model Parameters

Parameters that have biogeochemical meaning should reflect the patterns that characterize different ecosystem properties. Our mixed forest site (CN-mixed) generally showed intermediate parameter values compared to deciduous broadleaf and evergreen needleleaf forests (Figure 4). Some parameters exhibited distinct patterns among deciduous broadleaf and evergreen needleleaf forests. For instance, microbial maintenance respiration (m_R) was overall higher in evergreen needleleaf forests than in deciduous broadleaf forests (Figure 4c), but the opposite was seen for the initial active fraction (Figure 4l), indicating more stressed soil environment and higher energy limitation for microorganisms in evergreen needleleaf forests due to less substrate availability and poorer substrate quality. For other parameters, especially microbial- and enzyme-related parameters, the differences between the two major forest types were not significant (Figures 4f–4i). The half-saturation constant (K_m) is highest in the US-MOz site (Figure 4e), because it has the highest SOC content and the Michaelis-Menten formulation in the SOC enzymatic decay process requires a high K_m to maintain the relative substrate level within a reasonable range (otherwise the decay rate will be too fast,

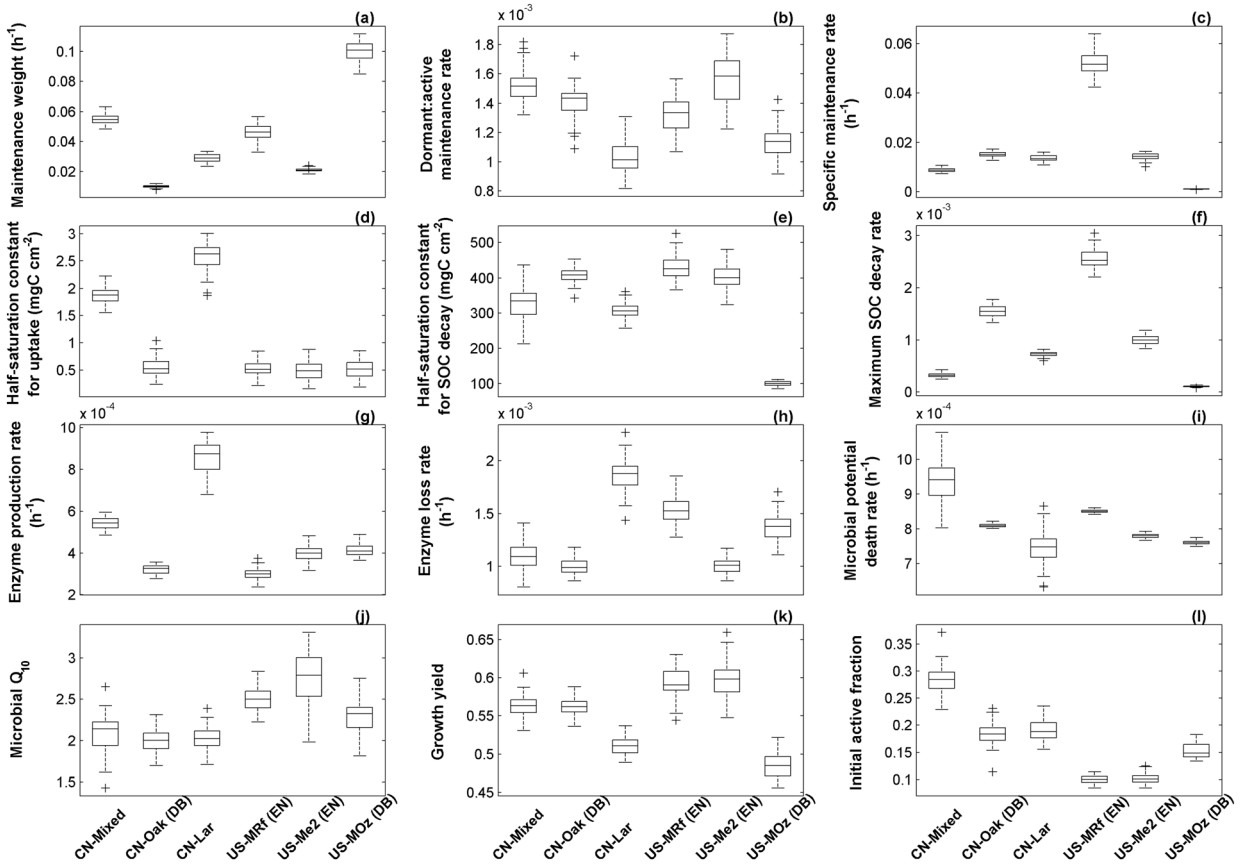

Figure 4. Boxplot of parameter posterior distribution that are obtained after ensemble inverse modeling for the dormancy model at all six sites. DB indicates deciduous broadleaf forest; EN indicates evergreen needleleaf forest. More details on the parameter description in the figure refer to Table 1.

i.e., substrate saturation; equation (1)). This also suggests the high sensitivity of the half-saturation constant to SOC in the Michaelis-Menten formulation.

3.3. Spatial Extrapolation

3.3.1. Spatial Distribution of Soil R_H and Microbial Biomass

The two models both simulated soil R_H ranging between 300 and 1000 g C m^{-2} yr^{-1}. The spatial pattern of the soil R_H of the dormancy and no dormancy models differed in large areas of northeastern U.S. and in southern China, with the no dormancy model simulating about 30% higher respiration than that of the dormancy model (Figures 5a and 5b). The soil R_H of other regions was generally comparable between the two models. The total soil R_H of all temperate forests from the dormancy model amounted to 7.28 Pg C yr^{-1} and 8.83 Pg C yr^{-1} from the no dormancy model. While there was no significant difference in the simulated spatial soil R_H between the models, the MIC/SOC ratio showed distinct patterns in both magnitude and spatial distribution of the two models (Figures 5c and 5d). Here the MIC represented the total microbial biomass including both active and dormant microorganisms for the dormancy model. The no dormancy model overall simulated about two times higher MIC/SOC ratio for temperate forests, especially in northern U.S., southern Europe, and northeastern China, than the dormancy model. In the no dormancy model, the MIC/SOC ratio can reach about 4% (Figure 5d), whereas in the dormancy model the ratio ranged from 0.5% to 2% (Figure 5c). Grid cell-based spatial correlation analysis showed that in both models, soil R_H was negatively affected by bulk density and particle density (Table 4, $\rho \approx 0.25$, $p < 0.001$) but had a significant correlation with soil C:N ratio ($\rho \approx 0.3$, $p < 0.001$) and especially organic matter content ($\rho \approx 0.5$, $p < 0.001$). In particular, our simulated spatial soil R_H of temperate forests was high at the Great Lakes regions in the U.S. where SOC content was also reported to be high from the GSDE data set (Figures 5a and 5b). Soil temperature and moisture also had significant positive effects on soil R_H ($\rho \approx 0.3$ and -0.1, respectively, $p < 0.001$) but were not as strong as the SOC.

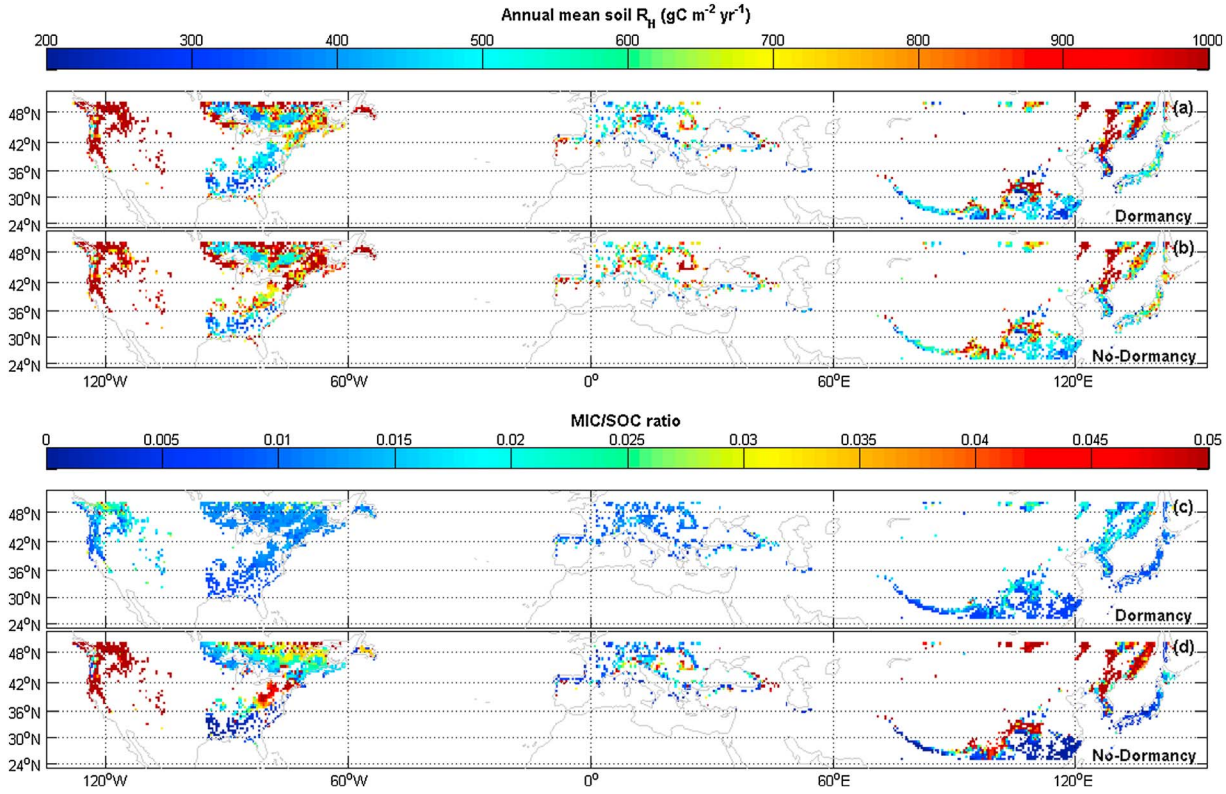

Figure 5. Simulated spatial pattern of (a) soil heterotrophic respiration (R_H) and (b) the MIC/SOC (total microbial biomass carbon to soil organic carbon) ratio of the two models.

3.3.2. Spatial Pattern of Microbial Dormancy and Its Controlling Factors

The annual active portion of microbial biomass ranged from 2% to 20% across temperate forests (Figures 6a and 6b). The spatial distribution of the active fraction of microbial biomass was relatively the same across seasons. The seasonal active portion of microbial biomass in summer was generally higher than in winter for large areas of northern U.S. and northeastern China, whereas southern U.S., Europe, and southern

Table 4. Pearson Correlation Coefficient by Grid Cell Between Active Portion of Microbial Biomass (r) and Soil Heterotrophic Respiration (R_H) and Soil Properties, Soil Temperature, and Soil Volumetric Moisture Content for Temperate Forest

	Dormancy Model				No Dormancy Model
Soil Physical and Environmental Factors	r (Summer)	r (Winter)	r (Annual Mean)	R_H	R_H
Bulk Density (g cm^{-3})	-	-	-	−0.17***	−0.25***
Particle Density (g cm^{-3})	-	-	-	−0.26***	−0.39***
Organic C Content (mg cm^{-2}) in the Top 30 cm	0.03	0.04	0.03	0.40***	0.62***
Soil C:N Ratio	−0.43***	−0.58***	−0.53***	−0.42***	−0.21***
Litterfall C Input (g C m^{-2} yr^{-1})	-	-	-	0.08**	0.07**
Annual Mean Soil Temperature at 10 cm	−0.19***	−0.28***	−0.14***	0.33***	0.29***
Annual Mean Soil Volumetric Moisture at 10 cm	0.10***	0.12***	0.06**	−0.11**	−0.12***
Soil Volumetric Moisture in Summer	0.06*	0.07*	0.09**	-	
Soil Volumetric Moisture in Winter	0.08	0.09**	0.05	-	-
	r Seasonal Amplitude ($r_{summer} - r_{winter}$)				
Seasonal Amplitude of Soil Temperature (Summer-Winter)	0.18***		0.03	-	-
Seasonal Amplitude of Soil Volumetric Moisture (Summer-Winter)	0.22***		−0.13**	-	-

*Significant at $p < 0.1$;
**Significant at $p < 0.05$;
***Significant at $p < 0.001$.

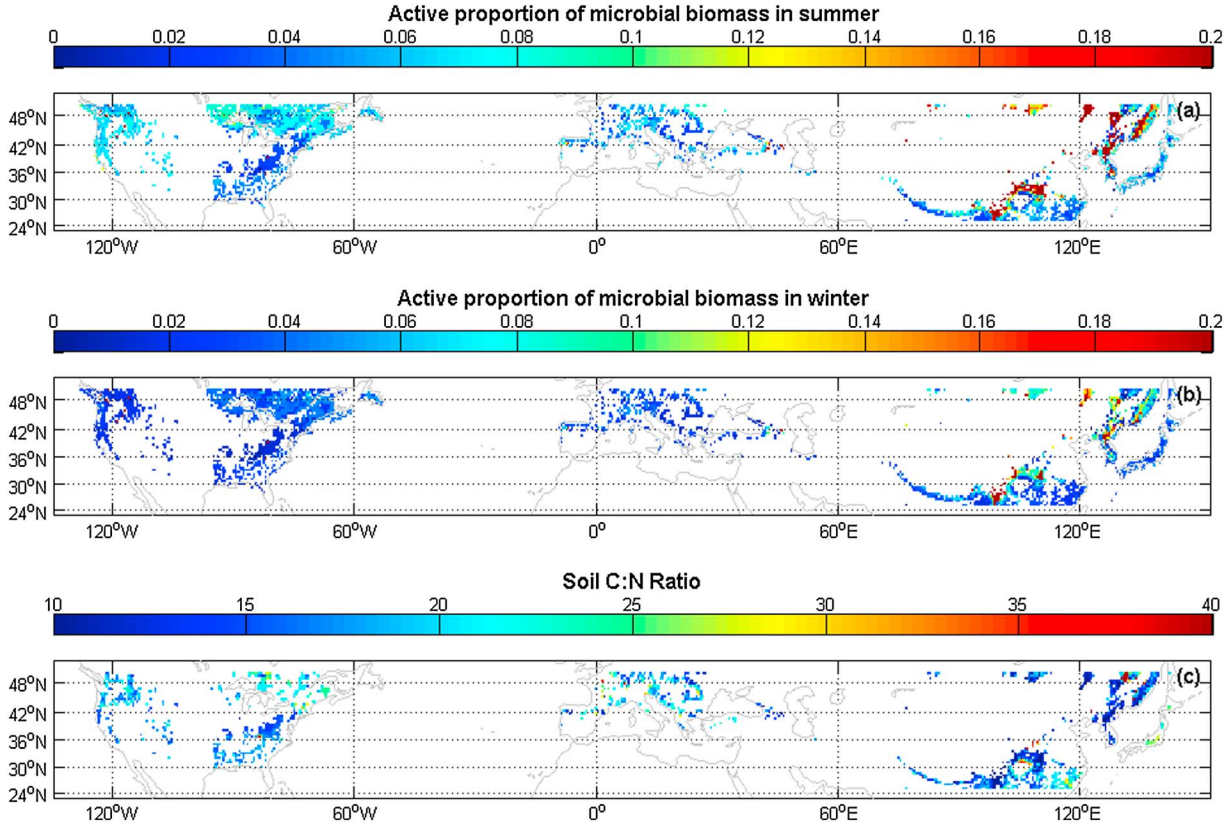

Figure 6. The spatial pattern of the active portion of microbial biomass in (a) summer and (b) winter and (c) the C:N ratio of soil organic matter of the temperate forest latitudinal band (25°N–50°N).

China featured a relatively constant active fraction across seasons (Figures 6a and 6b). Grid cell-based spatial correlation analysis showed that the soil C:N ratio was a major controlling factor on dormancy (Table 4, $\rho = -0.43$ in summer and -0.58 in winter, respectively, $p < 0.001$), indicating that higher nutrient availability (lower C:N ratio) yields lower dormancy proportion (higher active fraction). Annual temperature and moisture were weak controls on the spatial dormancy pattern ($\rho \approx 0.15$) except that the winter active fraction had a

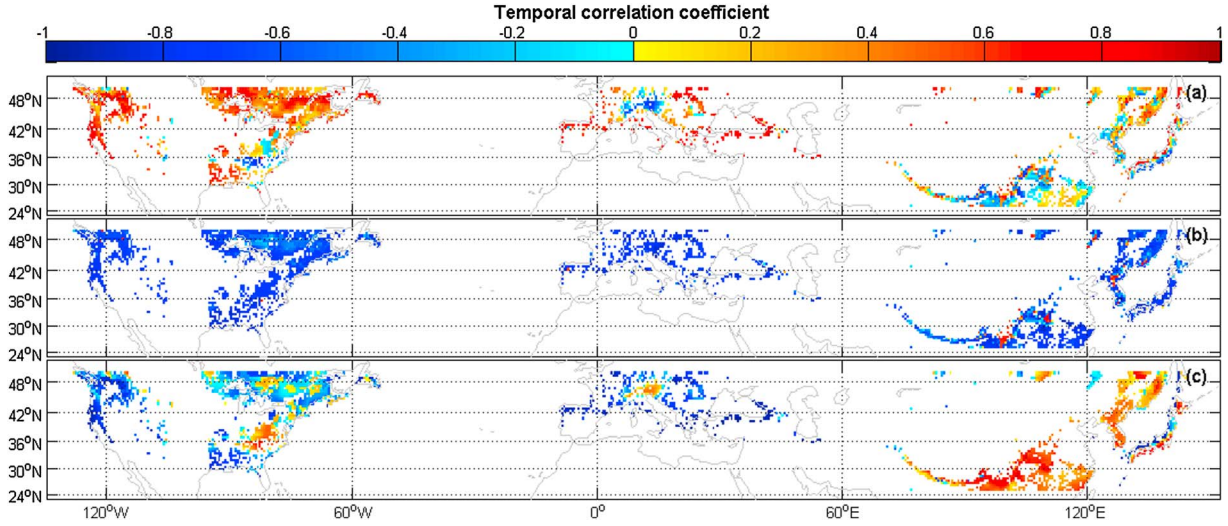

Figure 7. Temporal correlation (Pearson correlation coefficient) at each grid cell between the (a) active portion of microbial biomass and soil volumetric moisture content, (b) active portion of microbial biomass and soil temperature, and (c) soil temperature and moisture content.

slightly stronger negative correlation with annual temperature ($\rho = -0.28$, $p < 0.001$). However, temperature and moisture had very strong local controls on dormancy on temporal scales, with moisture having mostly strong positive temporal correlations with the active fraction ($\rho > 0.6$, Figure 7a), as moisture was formulated to directly control substrate availability. Temperature showed negative temporal correlation with the active fraction ($\rho < -0.5$, Figure 7b), primarily due to the negative covariation between temperature and moisture in the CCSM4 results (Figure 7c). It is worth noting here that, although annual temperature and moisture had weak controls on spatial patterns of active fraction, the seasonal amplitude of soil temperature and moisture generally exhibited higher correlations than that of the active fraction ($\rho > 0.18$ and $p < 0.001$, Table 4), suggesting high sensitivity of active-dormant transition to seasonal changes in moisture and temperature levels at large spatial scales.

4. Discussion

4.1. Model Performance and Limitations

A synthesis by *Bond-Lamberty et al*. [2004] documented soil R_H from temperate forests to range from 300 to 800 g C m^{-2} yr^{-1}. We calculated the regional total soil R_H based on the reported mean value of 600 g C m^{-2} yr^{-1} and the land cover map used in this study, resulting in a total soil R_H of around 7.11 Pg C yr^{-1}. The dormancy model produced closer estimates to this synthetic estimate with 7.5 ± 2.4 Pg C yr^{-1}, whereas the no dormancy model may overestimate soil R_H with 8.8 ± 3.5 Pg C yr^{-1}. Despite the comparable results between our simulated soil R_H and synthesized observations, our simplified modeling framework lacked explicit consideration of other nutrient cycles. Although we used soil C:N ratio to indicate substrate quality and its effects on microbial assimilation as a representative index, the coupled dynamics of kinetics and stoichiometric constraints on microbial physiology, which also pose key controls on decomposition dynamics, are not incorporated [*Sinsabaugh et al*., 2013]. While the simplified framework may be sufficient to serve the purpose of this study, a more complex modeling scheme that accounts for the stoichiometry of elements such as phosphorus should be able to reveal more biogeochemical controls which can then be benchmarked with observations to improve model performance.

Another caveat of our approach is that the model only simulates soils of the top 30 cm due to lack of microbial information below this depth. In the Chinese trenched plots, models simulated 20% drop in SOC over the course of 5 years. Although there was no C input at these sites, the SOC loss might still be overestimated because we attribute soil heterotrophic respiration from soils below 30 cm to that of the surface soil. In future model development, a depth-resolved modeling scheme and respiration measurements from the soil vertical profile would improve model realism (see discussion below).

4.2. Implications for Informing Experimental Needs

Rainfall-induced activation of dormant biomass can generate soil CO_2 pulses comparable in magnitude to the annual net C exchange of many terrestrial ecosystems (e.g., Mediterranean) [*Placella et al*., 2012; *Xu et al*., 2004]. Particularly, drying-rewetting events can exert stress on soil microbial communities and cause a decrease in soil basal respiration while total biomass increases [*Fierer and Schimel*, 2002]. In addition, changes in soil temperature and moisture conditions can induce responses in microbial basal respiration that were not explained by changes in total microbial biomass but rather changes in the physiology of soil microbial communities such as resuscitation of physiologically clustered microbial groups [*Hagerty et al*., 2014; *Placella et al*., 2012]. In contrast to seasonal variation in soil R_H driven by changes in temperature and moisture in a variety of ecosystems [*Suseela and Dukes*, 2013], total microbial biomass is generally unaffected by seasonality [*Blume et al*., 2002]. All of these indicate that soil respiration responses to environmental conditions are more closely associated with the active portion of microbial biomass than total microbial biomass. Thus, the no dormancy model that does not distinguish microbial biomass with different physiological states may not correctly represent the microbe-soil interactions. Similarly, using total biomass as an important metric in both experiments and modeling may also hinder effective data-model integration.

Our modeling results demonstrate that the ecosystem-level controls on dormancy at large spatial scales are different from that at local transient scales. This suggests that both site-level and spatial data should be used for model validation, because it is usually easier for models to reproduce site-level, short-term observations with data assimilation techniques, but much more difficult to capture spatial patterns [*Todd-Brown et al*., 2013] and long-term dynamics [*He et al*., 2014a]. In this study, we successfully reproduced soil R_H at six

temperature forest sites, but our extrapolated soil R_H revealed the potential issues with applying Michaelis-Menten kinetics on ecosystem scales and yielded high soil R_H in the northeastern U.S. due to the high SOC content in that region. Such insufficiency in the model structure may not be disclosed at site-level examination. Therefore, spatially gridded comprehensive soil C and microbial physiology metrics would be tremendously helpful in model validation and assessment. For example, the contrasting controls of bulk density, particle density, and organic C content on simulated soil R_H likely reflects covariation among these variables, because soil C concentration decreased with increasing particle density, implying less soil organic matter accumulation [*Sollins et al*., 2009]. Our simulated soil R_H is then able to reflect the spatial controls of soil physical properties on decomposition.

Uncertainty in driving data for decomposition models may also be substantial, and experimental measurements on large spatial scales would also be helpful. For example, the CCSM4 simulation we used cannot reproduce the surface frozen soil in northeastern China that we observed in the site-level measurements (Figure 3f), which potentially could introduce inaccuracies in model results. Note that in southern China broadleaf temperate forests do not show high temporal correlations of dormancy with soil moisture; this is likely because soil moisture is relatively constant throughout the year [*Tang et al*., 2006]; thus, soil moisture may not be the primary limiting factor on active fraction of microbial biomass in that region. More experimental data in that region should help benchmark both simulated soil moisture and temperature.

4.3. Implications for Informing Future Model Development

The high correlation between soil R_H and the organic C content in the top 30 cm (Table 4) in our analysis may be attributable to the Michaelis-Menten kinetics we used in the SOC enzymatic decay process (equation (1)), where SOC content directly controls saturation level of the organic matter. Michaelis-Menten kinetics has an implicit assumption that all substrates are accessible to enzymes under a homogeneous spatial distribution [*Michaelis and Menten*, 1913]. The soil solution-based measurements to which Michaelis-Menten kinetics usually apply are a good example that demonstrates the homogeneity requirement. In this way, Michaelis-Menten kinetics has a spatial limitation on relatively local scales (where homogeneous assumption holds). Nevertheless, the depth dependency of soil moisture, root inputs (e.g., root exudates and dead fine roots), and particle size in soils defies the underlying assumptions to Michaelis-Menten formulations.

Michaelis-Menten formulation also is derived under the assumption that enzymatic kinetics can cause a significant change in substrate levels [*Michaelis and Menten*, 1913], which is unrealistic for several soil processes influencing decomposition. For example, soil mineral-organic matter interaction and the occlusion of SOC by soil aggregates can form physical barriers to microbial extracellular hydrolysis of SOC [*Ayati*, 2012]. These limitations may explain the underperformance of both models, in particular the no dormancy model, at the US-MOz site, which has the lowest SOC content among the six sites. Although this issue is less notable in the dormancy model, the spatial distribution of high soil R_H in high SOC conditions still suggests some issues of using Michaelis-Menten kinetics when treating a large SOC as homogeneous (Table 4). We propose that a better representation of soil vertical heterogeneity [e.g., *Koven et al*., 2013] would be beneficial to using Michaelis-Menten kinetics in microbial-based decomposition models. Large SOC content likely induces mismatch of the temporal scale of SOC change with that of microbial activity. To reconcile the homogeneity assumption of Michaelis-Menten dynamics and the localization of actual SOC enzymatic decay, vertical heterogeneity can be implemented using multilayer soil model structure or depth-resolved SOC profile, thus ensuring a certain degree of homogeneity of SOC and enzyme distribution at each depth increment [*He et al*., 2014b]. Stabilization of organic matter by interaction with poorly crystalline minerals is also a key mechanism missing in current models [*Ayati*, 2012] and should be incorporated in future model development. In our model, the total SOC is used as substrate for enzymatic decay, when actually the active fraction of the organic matter should be used. In addition, it will be relatively easy to incorporate the moisture effects on enzyme activity into our models.

In both dormancy and nondormancy models, soil temperature and moisture exhibited similar levels of controls on soil R_H (Table 4). This is likely attributed to how soil moisture controls substrate availability within the model. As current first-order formulations in decomposition models only yield marginal effects of soil moisture [*Todd-Brown et al*., 2013], formulations with direct coupling between moisture and microbial activity should improve decomposition models.

5. Conclusion

Microbial life history traits such as dormancy play an important role in biogeochemical cycles. It has been widely observed that the active portion of microbial biomass, rather than the total biomass, explains the changes in microbial basal respiration rates. This study examines whether including dormancy in microbial-based soil decomposition model can improve the estimates of SOC dynamics and other microbial-related metrics. Our results showed that, although both dormancy and no dormancy models can capture the field-observed soil R_H, the no dormancy model exhibited larger seasonal oscillation and overestimated microbial biomass. Our regional modeling results also indicated that models with dormancy were able to produce more realistic magnitude of microbial biomass and soil R_H at both site-level and large spatial scales. Last, Michaelis-Menten kinetics may not be appropriate for models that do not vertically resolve decomposition dynamics in the soil profile. To be able to implement vertically resolved microbial processes, measurements of corresponding parameters from different ecosystems are imperative. This study also identified scale-dependent biogeochemical controls on microbial dynamics. Soil nutrient availability and quality, rather than seasonal variation of soil temperature and moisture, are the dominant control of spatial patterns of microbial dynamics. Overall, our findings suggest that future microbial model development should consider the representation of microbial dormancy, which will both improve the realism of microbial-based decomposition models and enhance the integration of soil experiments and mechanistically based modeling.

Acknowledgments

We would like to thank Xiaofeng Xu for his suggestions on an earlier version of this manuscript and Yang Bai for his helpful information regarding partitioning AmeriFlux data. We also would like to thank AmeriFlux PI Dr. Beverly Law for making these long-term observations publicly available. All data needed for reproduction of this study are available online (https://drive.google.com/folderview?id=0B081GsjCQ_JucnpQUGNyeU5hc-kk&usp=sharing) and also upon request. This research is partly supported with funding to Q.Z. through NSF projects (DEB-#0919331 and NSF-0630319), the NASA Land Use and Land Cover Change program (NASA-NNX09AI26G), Department of Energy (DE-FG02-08ER64599), and the NSF Division of Information & Intelligent Systems (NSF-1028291). Data from analyses and figures will be archived in the Purdue University Research Repository and can be accessed by contacting the corresponding author (Q.Z.). Any use of trade, firm, or product names is for descriptive purposes only and does not imply endorsement by the U.S. Government.

References

Allison, S. D., M. D. Wallenstein, and M. A. Bradford (2010), Soil-carbon response to warming dependent on microbial physiology, *Nat. Geosci.*, *3*(5), 336–340.

Ayati, B. P. (2012), Microbial dormancy in batch cultures as a function of substrate-dependent mortality, *J. Theor. Biol.*, *293*, 34–40.

Blagodatskaya, E., and Y. Kuzyakov (2013), Active microorganisms in soil: Critical review of estimation criteria and approaches, *Soil Biol. Biochem.*, *67*, 192–211.

Blume, E., M. Bischoff, J. Reichert, T. Moorman, A. Konopka, and R. Turco (2002), Surface and subsurface microbial biomass, community structure and metabolic activity as a function of soil depth and season, *Appl. Soil Ecol.*, *20*(3), 171–181.

Bond-Lamberty, B., C. Wang, and S. T. Gower (2004), A global relationship between the heterotrophic and autotrophic components of soil respiration?, *Global Change Biol.*, *10*(10), 1756–1766.

Cornelis, W. M., M. Khlosi, R. Hartmann, M. Van Meirvenne, and B. De Vos (2005), Comparison of unimodal analytical expressions for the soil-water retention curve, *Soil Sci. Soc. Am. J.*, *69*(6), 1902–1911.

Davidson, E. A., S. Samanta, S. S. Caramori, and K. Savage (2012), The dual Arrhenius and Michaelis-Menten kinetics model for decomposition of soil organic matter at hourly to seasonal time scales, *Global Change Biol.*, *18*(1), 371–384, doi:10.1111/j.1365-2486.2011.02546.x.

Duan, Q., S. Sorooshian, and V. K. Gupta (1994), Optimal use of the SCE-UA global optimization method for calibrating watershed models, *J. Hydrol.*, *158*(3–4), 265–284, doi:10.1016/0022-1694(94)90057-4.

Fierer, N., and J. P. Schimel (2002), Effects of drying-rewetting frequency on soil carbon and nitrogen transformations, *Soil Biol. Biochem.*, *34*(6), 777–787.

Fu, M., C. Wang, Y. Wang, and S. Liu (2009), Temporal and spatial patterns of soil nitrogen mineralization and nitrification in four temperate forests, *Acta Ecol. Sin.*, *29*(7), 3747–3758.

German, D. P., K. R. Marcelo, M. M. Stone, and S. D. Allison (2012), The Michaelis-Menten kinetics of soil extracellular enzymes in response to temperature: A cross-latitudinal study, *Global Change Biol.*, *18*(4), 1468–1479.

Hagerty, S. B., K. J. van Groenigen, S. D. Allison, B. A. Hungate, E. Schwartz, G. W. Koch, R. K. Kolka, and P. Dijkstra (2014), Accelerated microbial turnover but constant growth efficiency with warming in soil, *Nat. Clim. Change*, *4*(10), 903–906.

Hanson, P. J., N. T. Edwards, C. T. Garten, and J. A. Andrews (2000), Separating root and soil microbial contributions to soil respiration: A review of methods and observations, *Biogeochemistry*, *48*(1), 115–146, doi:10.1023/a:1006244819642.

He, Y., J. Yang, Q. Zhuang, A. D. McGuire, Q. Zhu, Y. Liu, and R. O. Teskey (2014a), Uncertainty in the fate of soil organic carbon: A comparison of three conceptually different decomposition models at a larch plantation, *J. Geophys. Res. Biogeosci.*, *119*, 1892–1905, doi:10.1002/2014jg002701.

He, Y., Q. Zhuang, J. W. Harden, A. D. McGuire, Z. Fan, Y. Liu, and K. P. Wickland (2014b), The implications of microbial and substrate limitation for the fates of carbon in different organic soil horizon types of boreal forest ecosystems: A mechanistically based model analysis, *Biogeosciences*, *11*(16), 4477–4491, doi:10.5194/bg-11-4477-2014.

IPCC (2013), Summary for policymakers, in *Climate Change 2013: The Physical Science Basis. Contribution of Working Group I to the Fifth Assessment Report of the Intergovernmental Panel on Climate Change Rep*, edited by T. F. Stocker et al., Cambridge Univ. Press, Cambridge, U. K., and New York.

Irvine, J., and B. E. Law (2002), Contrasting soil respiration in young and old-growth ponderosa pine forests, *Global Change Biol.*, *8*(12), 1183–1194, doi:10.1046/j.1365-2486.2002.00544.x.

Jobbágy, E. G., and R. B. Jackson (2000), The vertical distribution of soil organic carbon and its relation to climate and vegetation, *Ecol. Appl.*, *10*(2), 423–436, doi:10.1890/1051-0761(2000)010[0423:tvdoso]2.0.co;2.

Koven, C., W. Riley, Z. Subin, J. Tang, M. Torn, W. Collins, G. Bonan, D. Lawrence, and S. Swenson (2013), The effect of vertically resolved soil biogeochemistry and alternate soil C and N models on C dynamics of CLM4, *Biogeosciences*, *10*, 7109–7131.

Lasslop, G., M. Reichstein, D. Papale, A. D. Richardson, A. Arneth, A. Barr, P. Stoy, and G. Wohlfahrt (2010), Separation of net ecosystem exchange into assimilation and respiration using a light response curve approach: Critical issues and global evaluation, *Global Change Biol.*, *16*(1), 187–208, doi:10.1111/j.1365-2486.2009.02041.x.

Lennon, J. T., and S. E. Jones (2011), Microbial seed banks: The ecological and evolutionary implications of dormancy, *Nat. Rev. Microbiol.*, *9*(2), 119–130.

Li, J., G. Wang, S. Allison, M. Mayes, and Y. Luo (2014), Soil carbon sensitivity to temperature and carbon use efficiency compared across microbial-ecosystem models of varying complexity, *Biogeochemistry*, *119*, 67–84, doi:10.1007/s10533-013-9948-8.

Liu, S., and C. Wang (2010), Spatio-temporal patterns of soil microbial biomass carbon and nitrogen in five temperate forest ecosystems, *Acta Ecol. Sin.*, *30*(12), 3135–3143.

Manzoni, S., R. B. Jackson, J. A. Trofymow, and A. Porporato (2008), The global stoichiometry of litter nitrogen mineralization, *Science*, *321*(5889), 684–686, doi:10.1126/science.1159792.

McFarlane, K., M. Torn, P. Hanson, R. Porras, C. Swanston, M. Callaham Jr., and T. Guilderson (2013), Comparison of soil organic matter dynamics at five temperate deciduous forests with physical fractionation and radiocarbon measurements, *Biogeochemistry*, *112*(1–3), 457–476, doi:10.1007/s10533-012-9740-1.

Michaelis, L., and M. L. Menten (1913), The kinetics of the inversion effect, *Biochem. Z.*, *49*, 333–369.

Placella, S. A., E. L. Brodie, and M. K. Firestone (2012), Rainfall-induced carbon dioxide pulses result from sequential resuscitation of phylogenetically clustered microbial groups, *Proc. Natl. Acad. Sci. U.S.A.*, *109*(27), 10,931–10,936.

Purich, D. L. (2009), *Contemporary Enzyme Kinetics and Mechanism: Reliable Lab Solutions*, Academic Press, Oxford, U. K.

Raich, J. W., and C. S. Potter (1995), Global patterns of carbon-dioxide emissions from soils, *Global Biogeochem. Cycles*, *9*(1), 23–36, doi:10.1029/94GB02723.

Schimel, J. P., and M. N. Weintraub (2003), The implications of exoenzyme activity on microbial carbon and nitrogen limitation in soil: A theoretical model, *Soil Biol. Biochem.*, *35*(4), 549–563, doi:10.1016/s0038-0717(03)00015-4.

Shangguan, W., Y. Dai, Q. Duan, B. Liu, and H. Yuan (2014), A global soil data set for earth system modeling, *J. Adv. Model. Earth Syst.*, *6*(1), 249–263, doi:10.1002/2013ms000293.

Sinsabaugh, R. L., S. Manzoni, D. L. Moorhead, and A. Richter (2013), Carbon use efficiency of microbial communities: Stoichiometry, methodology and modelling, *Ecol. Lett.*, *16*(7), 930–939, doi:10.1111/ele.12113.

Sollins, P., M. Kramer, C. Swanston, K. Lajtha, T. Filley, A. Aufdenkampe, R. Wagai, and R. Bowden (2009), Sequential density fractionation across soils of contrasting mineralogy: Evidence for both microbial- and mineral-controlled soil organic matter stabilization, *Biogeochemistry*, *96*(1–3), 209–231, doi:10.1007/s10533-009-9359-z.

Suseela, V., and J. S. Dukes (2013), The responses of soil and rhizosphere respiration to simulated climatic changes vary by season, *Ecology*, *94*, 403–413.

Tang, X., S. Liu, G. Zhou, D. Zhang, and C. Zhou (2006), Soil-atmospheric exchange of CO_2, CH_4, and N_2O in three subtropical forest ecosystems in southern China, *Global Change Biol.*, *12*(3), 546–560.

Thomas, C. K., B. E. Law, J. Irvine, J. G. Martin, J. C. Pettijohn, and K. J. Davis (2009), Seasonal hydrology explains interannual and seasonal variation in carbon and water exchange in a semiarid mature ponderosa pine forest in central Oregon, *J. Geophys. Res.*, *114*, G04006, doi:10.1029/2009JG001010.

Todd-Brown, K. E. O., J. T. Randerson, W. M. Post, F. M. Hoffman, C. Tarnocai, E. A. G. Schuur, and S. D. Allison (2013), Causes of variation in soil carbon simulations from CMIP5 Earth system models and comparison with observations, *Biogeosciences*, *10*(3), 1717–1736, doi:10.5194/bg-10-1717-2013.

Wang, C., J. Yang, and Q. Zhang (2006), Soil respiration in six temperate forests in China, *Global Change Biol.*, *12*(11), 2103–2114.

Wang, G., M. A. Mayes, L. Gu, and C. W. Schadt (2014), Representation of dormant and active microbial dynamics for ecosystem modeling, *PLoS One*, *9*(2), e89252, doi:10.1371/journal.pone.0089252.

Wang, T., A. Hamann, D. Spittlehouse, and S. Aitken (2006), Development of scale-free climate data for Western Canada for use in resource management, *Int. J. Climatol.*, *26*(3), 383–397.

Wang, Y., B. Chen, W. Wieder, M. Leite, B. Medlyn, M. Rasmussen, M. Smith, F. B. Agusto, F. Hoffman, and Y. Luo (2014), Oscillatory behavior of two nonlinear microbial models of soil carbon decomposition, *Biogeosciences*, *11*(7), 1817–1831.

Wieder, W. R., G. B. Bonan, and S. D. Allison (2013), Global soil carbon projections are improved by modelling microbial processes, *Nat. Clim. Change*, *3*(10), 909–912.

Wirtz, K. W. (2003), Control of biogeochemical cycling by mobility and metabolic strategies of microbes in the sediments: An integrated model study, *FEMS Microbiol. Ecol.*, *46*(3), 295–306.

Xu, L., D. D. Baldocchi, and J. Tang (2004), How soil moisture, rain pulses, and growth alter the response of ecosystem respiration to temperature, *Global Biogeochem. Cycles*, *18*, GB4002, doi:10.1029/2004GB002281.

Xu, X., P. E. Thornton, and W. M. Post (2013), A global analysis of soil microbial biomass carbon, nitrogen and phosphorus in terrestrial ecosystems, *Global Ecol. Biogeogr.*, *22*(6), 737–749.

Xu, X., J. P. Schimel, P. E. Thornton, X. Song, F. Yuan, and S. Goswami (2014), Substrate and environmental controls on microbial assimilation of soil organic carbon: A framework for Earth system models, *Ecol. Lett.*, *17*(5), 547–555.

Yang, J., and C. Wang (2005), Soil carbon storage and flux of temperate forest ecosystems in northeastern China, *Acta Ecol. Sin.*, *25*(11), 2875–2882.

Yvon-Durocher, G., J. M. Caffrey, A. Cescatti, M. Dossena, P. del Giorgio, J. M. Gasol, J. M. Montoya, J. Pumpanen, P. A. Staehr, and M. Trimmer (2012), Reconciling the temperature dependence of respiration across timescales and ecosystem types, *Nature*, *487*(7408), 472–476.

Zhao, M., and S. W. Running (2010), Drought-induced reduction in global terrestrial net primary production from 2000 through 2009, *Science*, *329*(5994), 940–943.